Journal of Materials Chemistry C

ROYAL SOCIETY OF CHEMISTRY

COMMUNICATION

View Article Online
View Journal | View Issue

Check for updates

Cite this: J. Mater. Chem. C, 2024, 12, 1625

Received 9th August 2023,
Accepted 19th December 2023

DOI: 10.1039/d3tc02849f

rsc.li/materials-c

The impact of hydrogen peroxide production in OECTs for *in vitro* applications†

Claudia Lubrano,‡[abc] Ottavia Bettucci,§‡[c] Gerwin Dijk,[d] Alberto Salleo,[d] Alexander Giovannitti¶*[d] and Francesca Santoro*[abc]

Organic electrochemical transistors (OECTs) have shown great potential in bioelectronics to transduce small biological signals for applications such as the electrical recording of excitable cells and assessing cell barrier properties. It is imperative that operating the OECT as a biosensor does not affect the biological system. However, bias voltages applied to channel materials such as the conducting polymer (CP) PEDOT:PSS have been shown to induce the formation of hydrogen peroxide (H_2O_2) which can disrupt the physiology of cells. In this work, we evaluated the impact of H_2O_2 formation during OECT operation by comparing an oxygen-sensitive CP (PEDOT:PSS) and an oxygen-stable CP (p(gPyDPP-MeOT2)). While both CPs show high biocompatibility in their non-biased, resting state, we observed large differences during the operation of the electrochemical device. OECTs with PEDOT:PSS produce H_2O_2 where the H_2O_2 concentration in the electrolyte depends on the channel area and the time of operation. In comparison, OECTs using the oxygen-stable DPP-based polymer showed no sign of H_2O_2 formation. Further investigation also revealed how the proliferation rate of neuronal cells directly interfaced with such OECTs was affected by the concentration of H_2O_2. Our work demonstrated the limitations of oxygen-sensitive OECT channel materials for bioelectronic applications and provides guidance for material design strategies to develop safe bioelectronic devices for real-life applications.

Introduction

Recent advances in the synthesis of semiconducting polymers have greatly enhanced the performance of organic electrochemical transistors (OECTs).[1,2] OECTs function in aqueous electrolytes which enable the use of these devices for health monitoring and to interphase with biological systems.[3] Moreover, OECTs have high transconductances (g_m) which enables the amplification/transduction of low-voltage biological signals into electric signals.[2,4] Examples of employing OECTs for bioelectronic applications include the recording of electroactive cells, impedance sensing to assess cell barrier properties, and the detection of analytes.[5–9] The OECT operating mechanism is described in several recent studies and will thus not be discussed in detail in this work.[10,11] The OECT performance strongly depends on the choice of the channel material, the device dimension, and the operational voltage.[12]

Typically, the channel material consists of an organic mixed ionic-electronic conductor (OMIEC)[11] which is designed to simultaneously transport electronic and ionic charge carriers for efficient signal transduction. In contact with aqueous electrolytes, solvent molecules, and ions can migrate into the bulk of the channel material (swelling) which opens the structure of the polymer to enable ion penetration into the bulk of the polymer. Furthermore, upon applying an electrochemical potential with respect to the gate (or reference) electrode (Ag/AgCl), electronic charges are injected into the OMIEC and ions migrate from the electrolyte into the bulk of the OMIEC to compensate for the electronic charges injected into the system. Conventionally, the performance of OECTs is benchmarked by the product of the electronic mobility (μ) and the volumetric charge storage capacitance (C^*), which are used to calculate the transconductance of the transistor.[13] Although the transconductance is an important figure of merit, it only defines the amplification of the device and does not include other aspects such as biocompatibility, electrochemical side reactions, and operational stability. While some work described the operational stability of devices,[14] little work has been carried out on

[a] Institute of Biological Information Processing – Bioelectronics, IBI-3, Forschungszentrum Juelich, 52428, Germany. E-mail: francesca.santoro@iit.it
[b] Faculty of Electrical Engineering and IT, RWTH Aachen, 52074, Germany
[c] Tissue Electronics, Istituto Italiano di Tecnologia, 80125, Naples, Italy
[d] Department of Materials Science and Engineering, Stanford University, Stanford, CA, USA. E-mail: alexander.giovannitti@chalmers.se

† Electronic supplementary information (ESI) available. See DOI: https://doi.org/10.1039/d3tc02849f

‡ Equal contribution.

§ Current address: Department of Materials Science and Milano-Bicocca Solar Energy Research Center – MIB-Solar, University of Milano-Bicocca, 20125 Milano, Italy.

¶ Current address: Department of Chemistry and Chemical Engineering, Chalmers University of Technology, Göteborg 412 96, Sweden.

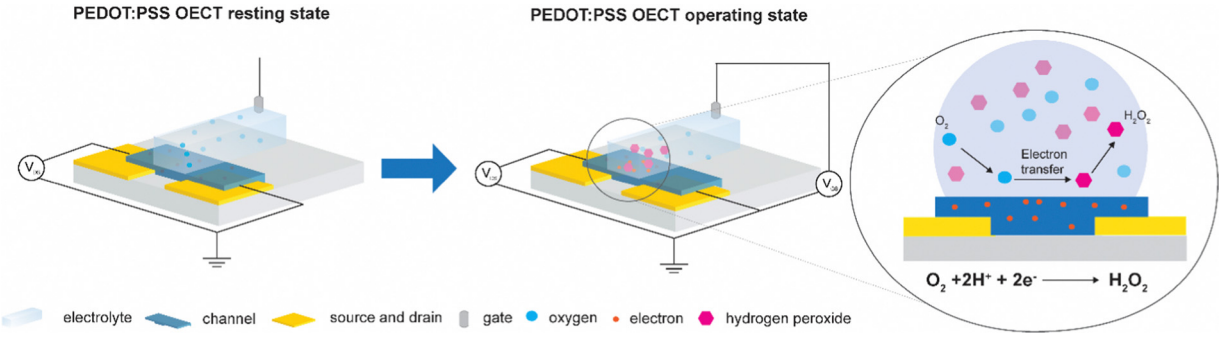

Fig. 1 A schematics of PEDOT:PSS OECT in its resting state and upon V_g operation, showing electron transfer from the polymer channel to the electrolyte and consequent generation of H_2O_2.

investigating the impact of electrochemical side reactions (faradaic reactions) during device operation, forming reactive side products that may be harmful to biological systems.

Currently, PEDOT:PSS is the most used channel material as it achieves high transconductance and is commercially available.[15] However, recent reports have demonstrated that OECTs and electrodes based on PEDOT:PSS form hydrogen peroxide (H_2O_2) during operation in oxygenated aqueous electrolytes[16–20] (Fig. 1). These electrochemical side reactions are expected to cause degradation of the transistor material and importantly, also affect the health of cells that are in contact with the device. H_2O_2 is a reactive oxygen species that plays an essential role in the physiology of cells and tissue.[21–23] It is generated naturally through metabolic activity and can diffuse across cellular membranes to act as a molecule messenger and establish redox signaling that initiates direct cellular effects such as changes in shape, proliferation, and differentiation. Under normal conditions, living organisms exhibit antioxidant systems that balance the generation and elimination of hydrogen peroxide. However, external factors can for instance facilitate oxidative stress that disrupts the redox signaling and damages biomolecules such as DNA, proteins, and lipids ultimately leading to cell death.[24–26] Furthermore, the oxygen reduction reaction (ORR) can disrupt the cell physiology and deplete oxygen in the electrolyte which may lead to hypoxia for cells near the device. Thus, to engineer inert bioelectronic devices for real-life applications, oxygen-stable OECT materials are needed that function without faradaic side reactions with molecular oxygen to limit the accumulation of H_2O_2 during device operation.

In this work, we evaluated the impact of H_2O_2 formation during OECT operation in oxygen-containing aqueous electrolytes by comparing an oxygen-sensitive OMIEC (PEDOT:PSS) to an oxygen-stable OMIEC (p(gPyDPP-MeOT2)). For each channel material, the generated H_2O_2 concentration was determined and the viability of neurons that were exposed to peroxide containing electrolytes was examined. Furthermore, neurons cultured on a PEDOT:PSS channel were visually inspected before and after OECT operation.

Results and discussion

To investigate if H_2O_2 was formed during device operation and to quantify the amount of H_2O_2 formed on the channel of the OECT, we prepared OECTs with a defined area and operated them in ambient conditions. First, transfer curves were measured for the two different polymers (Fig. S1, ESI†) to characterize their mode of operation. The oxygen-sensitive polymer, PEDOT:PSS, operated in depletion mode where the polymer was initially in its conductive state and scanning the gate potential to positive values results in reduction of the polymer, switching the device to its off state. The discharged PEDOT:PSS was reactive and oxidized in the presence of molecular oxygen forming H_2O_2, as illustrated in Fig. 1. In comparison, the oxygen-stable polymer p(gPyDPP-MeOT2) operated in enhancement mode. The polymer had a low electronic conductivity (device begins in off state) and sweeping the gate potential to negative values induced an oxidation of the polymer that increases the electronic conductivity and switches the device to its on state. As previously reported, both the neutral and oxidized states of the polymer were not reactive towards molecular oxygen.[18,27,28] To quantify the amount of H_2O_2 that is generated and assess the effect on cells, devices were operated by applying gate voltage pulses V_g (with fixed channel voltages, V_d) in ambient conditions, repeatedly switching the devices between the off and on state. The faradaic side reactions of the devices were then investigated by monitoring the gate current of the OECT.

The amount of hydrogen peroxide formation during the operation of the devices was measured with a colorimetric assay. In the presence of hydrogen peroxide, the horseradish peroxidase (HRP) catalyzed the conversion of the fluorescent probe into a colorimetric product that changed the absorbance spectra of the solution. A calibration curve was used to determine the concentration of hydrogen peroxide generated during the operation of the OECTs (Fig. S2, ESI†). Operating the PEDOT:PSS OECT at peak g_m (V_g = 700 mV *vs.* Ag/AgCl, with V_d = −500 mV) for 60 seconds caused generation of H_2O_2 in the electrolyte ranging from 20 to 50 μM (Fig. 2a). On the contrary, no hydrogen peroxide was detected (considering the experimental concentration limit of 5 μM) in the electrolyte of the OECT using polymer p(gPyDPP-MeOT2) (Fig. 2b). For the PEDOT:PSS OECTs, the concentration of generated H_2O_2 was determined for different durations of the applied gate potential as well as for different channel dimensions. OECTs with millimeter and micrometer scale dimensions were operated for 1

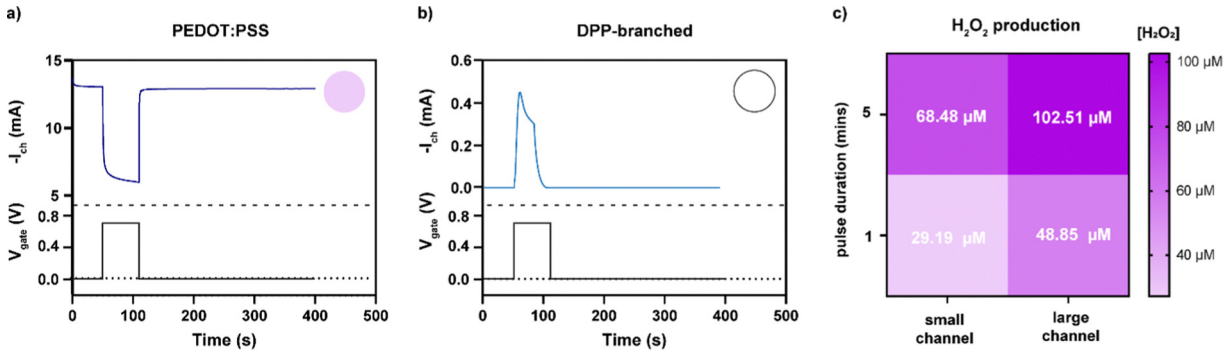

Fig. 2 Current response of the OECT with (a) PEDOT:PSS and (b) p(gPyDPP-MeOT2) upon applying a square voltage pulse at the gate electrode (V_g = 700 mV, and V_d = −500 mV for PEDOT:PSS, V_g = −700 mV, and V_d = −100 mV for p(gPyDPP-MeOT2)). The circular insets show the concentration of peroxide recalling the same color code reported in Fig. 3c. Degradation of p(gPyDPP-MeOT2) is observed at potentials > −650 mV.[14] (c) Color map representing the concentration of H_2O_2 (expressed in µM) produced during the operation of a PEDOT:PSS OECT for different channel areas and gate pulse duration.

and 5 minutes and the colorimetric assay was used to determine the H_2O_2 concentration (color map in Fig. 2c). We observed the highest concentration of H_2O_2 for the large OECT (7 × 4 mm^2) when a long gate pulse (5 minutes) was applied indicating that the H_2O_2 formation depended on the active area of the device and the operation time. The number of charges injected from the gate electrode into the polymer channel correlated to the generated concentration of H_2O_2, confirming that the by-products from the electrochemical reactions were directly related to the biasing of the OECT (Fig. S3, ESI†).

The biocompatibility of both polymers was first assessed in their unbiased state (*i.e.*, no gate voltage was applied), by cultivating neuronal cells (HT22) on polymer films and using a live/dead fluorescence assay. After 24 hours in culture, high percentages of green fluorescent cells (>95%) were found indicating excellent viability on both PEDOT:PSS and p(gPyDPP-MeOT2) (Fig. 3a(i)–(iii)). No significant difference in the percentage of live cells was found compared to the glass substrate control, suggesting negligible cytotoxic effects (Fig. 3b). To determine whether the amount of peroxide produced during PEDOT:PSS-based OECT operation affected the cell viability, two concentrations of H_2O_2 (20 µM and 100 µM) were tested, corresponding to the amount of peroxide produced with large channel area-long pulse duration and small channel area-short pulse duration, respectively. After 1 day from plating, HT22 cells were exposed to hydrogen peroxide by exchanging

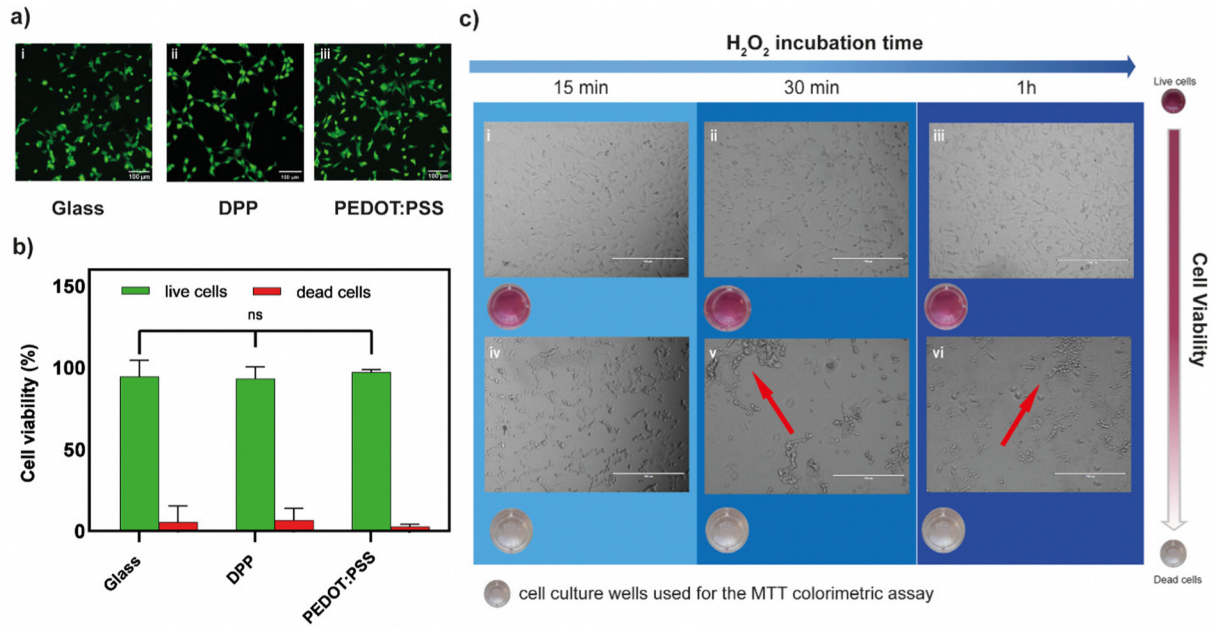

Fig. 3 (a) HT22 cell viability (60 000 cell per cm^2) assay showing fluorescently labeled live (green) and dead (red) cells on glass (i), p(gPyDPP-MeOT2) polymer (ii) and PEDOT:PSS (iii). (b) Percentage of live and dead cells reported as mean ± SEM (n = 3). (c) Brightfield images of HT22 cells seeded on glass at different time points (15, 30, and 60 min) without (i)–(iii) and with (iv)–(vi) 100 µM H_2O_2 produced by operating the OECT. The circles are the MTT coloring indicating cell viability (pink: live cells, transparent: dead cells) and the red arrows locate cells clusters that were formed. Scale bar: 100 µm.

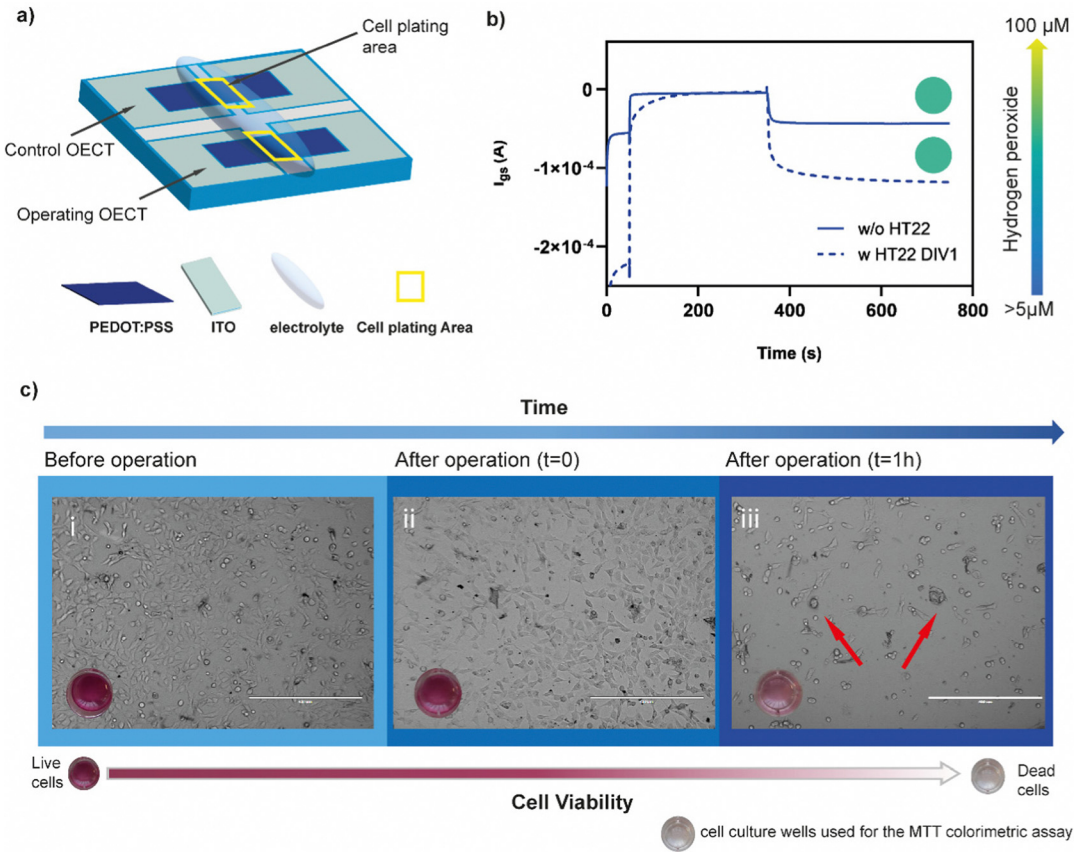

Fig. 4 (a) OECT device on a glass substrate with ITO contacts (source and drain) and two spin coated PEDOT:PSS channels. Each glass substrate contained two OECTs (cell plating area 5 mm^2). One OECT was used as a control (no voltage is applied during the experiment) and the other OECT is operated (by applying 700 mV). (b) Output channel current upon the application of a 5 min square voltage pulse at the gate with and without cells (dotted and solid line, respectively). (c) Brightfield images of the HT22 cell line before operation (i), directly after applying the voltage pulse (ii) and after 1 h from applying the voltage pulse (iii). Red arrows pointing at cells clusters that were formed. Scale bar: 100 µm.

the cell medium with H_2O_2-containing medium at the desired concentration after which the metabolic activity was evaluated at different time points through an MTT assay. At low H_2O_2 concentration (20 µM), a slight decrease in the metabolic activity was observed that was proportionally related to the exposure time to H_2O_2 (Fig. S4, ESI†). Increasing the H_2O_2 concentration to 100 µM showed a large change in the absorbance values after 15 minutes, indicating a significant decrease in the metabolic activity of cells (Fig. S4 (ESI†) and Fig. 3c). This was further confirmed by a change in the cell shape as well as by the presence of cell clusters (Fig. 3c(iv)–(vi)). These results demonstrated the sensitivity of HT22 cells hydrogen peroxide produced concentrations during the transistor operation.

To evaluate whether the presence of cells might affect the production of hydrogen peroxide protecting the polymer form undergoing the ORR, HT22 cells were cultivated (60 000 cell per cm^2) on top of a PEDOT:PSS OECT, covering the channel area (Fig. 4a). The device was operated at V_g = 700 mV and V_d = −500 mV for 5 minutes. Comparing the amount of H_2O_2 produced before and after cell plating, no significant difference was found ($\lambda_{570before}$ = 0.111 ± 0.011 $\lambda_{570after}$ = 0.099 ± 0.020, n = 3) suggesting that the presence of cells is not limiting the generation, diffusion and detection of peroxide (Fig. 4b).

After device operation, cells were incubated for 1 hour in the same media. The absorbance values evaluated through MTT assay indicated a drastic decrease in the metabolic activity of the HT22 (λ_{570} = 0.122) with respect to the control (λ_{570} = 0.348) (not operated device) (Fig. 4c). Similar results were found with 3 different devices (Fig. S5, ESI†). Brightfield images showed round-shaped morphology and cluster formation confirming the adverse effects of oxidative stress on the cells physiology.

Conclusions

In this work, we demonstrated the impact of hydrogen peroxide generated by OECTs on neuronal cells for two distinguished OMIEC materials. Cells proliferation rate was not altered when seeded on the unbiased OMIECs, showing the non-toxic nature of the OMIECs. However, when operating the oxygen-sensitive OMIEC in electrochemical transistors, the production of cytotoxic hydrogen peroxide was observed which significantly affected the cell viability. We observed a strong correlation between the amount of hydrogen peroxide produced and the

duration of the applied potential as well as the channel area of the device. Importantly, operating OECTs with PEDOT:PSS (channel area of 28 mm^2) formed up to 100 μM of H_2O_2 after operating the device for 5 minutes, which strongly impacted the physiology of the cells. In comparison, the oxygen-stable (p(gPyDPP-MeOT2)) showed no sign of H_2O_2 formation during operation at peak transconductance, paving the way for the development of safe bioelectronic devices. Future materials design for OECTs should therefore not merely focus on increasing the transconductance, but also consider the electrochemical reactions and resulting byproducts to support the development of safer bioelectronic devices.

Experimental section

Materials

PEDOT:PSS was purchased from Clevios (PH 1000, Merck Life Science S.r.l., Italy). Polymer p(gPyDPP-$MeOT_2$) based on pyridine-flanked diketopyrrolopyrrole (PyDPP) with bithiophene (T2) or 3,3′-methoxybithiophene (MeOT2) were synthesized by a Stille polymerization as previously described.[18]

Large organic electrochemical transistor fabrication

A two-squared patterned ITO coated glass (surface resistivity 20 Ω cm^{-2}, 25 mm × 12.5 mm, Xinyan Technology Ltd, Hong Kong) was cleaned with deionized water, acetone (Merck Life Science S.r.l., Italy), and 2-propanol (Merck Life Science S.r.l., Italy) (10 minutes for each solvent) and dried with compressed air. Then, the ITO glass underwent a plasma activation (2 minutes, 20 W) to favor the spin coating of a previously prepared PEDOT:PSS aqueous solution (5 vol% ethylene glycol (Merck Life Science S.r.l., Italy), 0.002 vol% DBSA (Merck Life Science S.r.l., Italy), and 1 vol% GOPS (Merck Life Science S.r.l., Italy) added to a commercial Hereaus Clevios PH1000) that was sonicated 30 minutes before use. The PEDOT:PSS was spin coated at 2000 rpm for 2 minutes with an acceleration of 400 rpm and annealed 1 hour at 140 °C. Finally, to pattern the PEDOT:PSS channel area, a plasma etching (15 minutes, 100 W) was performed covering the PEDOT strip with a Polydimethylsiloxane (PDMS) masks (15 mm × 7 mm) to form a (28 mm^2 channel). Later, the OECT was left in deionized water overnight to promote the PEDOT:PSS swelling.

Small organic electrochemical transistor fabrication

Interdigitated electrodes (Micrux, 15 pairs of electrodes with W = 1950 μm, L = 10 μm) were cleaned by sonication for 15 minutes in acetone and isopropanol, followed by an ozone treatment for 5 minutes. Devices were prepared by spin coating polymer solution. For PEDOT:PSS, the above-described solution mixture was spin coated at 3000 rpm, followed by an annealing step at 120 °C for 15 minutes. The device was rinsed with DI water and dried before testing. For polymer p(gPyDPP-MeOT2), a polymer solution was prepared by dissolving the polymer in chloroform (10 mg mL^{-1}). The polymer solution was filtered with a 0.45 μm filter and spin cast at 1000 rpm without further thermal treatment. The area of the devices was defined by removing the polymer manually with a sharp blade.

OECT operation

Following characterizations have been performed by using a commercial platform (ARKEO, Cicci Research, Italy).

Transfer-characteristic. Devices were characterized by using two measurement probes connected to the source and drain electrodes and a third one connected to the Ag/AgCl gate electrode. Transfer curves were taken by sweeping the gate voltage from −0.8 V to 0.8 V with a scan rate of 50 mV s^{-1} and the drain voltage (both *versus* the source potential) from −0.6 V to 0.1 V with a scan rate of 50 mV s^{-1}.

Pulsed measurements. Pulsed measurements on devices were performed by using the previous platform and setup, keeping a fixed drain voltage of V_{ds} = −500 mV a voltage square pulse at the gate electrode (PW = 5 min, V_g = 700 mV).

Peroxide essay

To evaluate the amount of peroxide produced during the transistor operation the Peroxidase Activity Assay Kit (Merck Life Science S.r.l., Italy) has been used exploiting the capability of peroxidase to catalyzes the reaction between H_2O_2 and a fluorescent probe, resulting in a colorimetric (570 nm) product, proportional to the peroxidase activity present. One unit of peroxidase is defined as the amount of enzyme that reduces 1.0 μmole of H_2O_2 per minute at 37 °C. After operating the device, the electrolyte has been removed and developed in another vial with the appropriate amount of reagent following the protocol reported in the commercial kit. The solution was then measured spectrophotometrically using Dynatech MR580 Microelisa reader, using a test wavelength of 570 nm.

Cell culture, biocompatibility, and viability essay

Live-dead assay. The experiments were performed using HT22 cells (ATCC, Italy), an immortalized mouse hippocampal cell line. HT22 cells were cultured in 25 mm^2 flask in DMEM:F-12 (1 : 1) media (Merck Life Science S.r.l., Italy) supplemented with 10% fetal bovine serum (Merck Life Science S.r.l., Italy), 1% penicillin/streptomycin (Merck Life Science S.r.l., Italy), 1% L-glutamine (Merck Life Science S.r.l., Italy), in a 5% CO_2 incubator at 37 °C. Confluent HT22 cells were trypsinated using Trypsin-EDTA 0.25% (Life Technologies Italia, Italy) and cells were seeded on the polymeric substrates at a density of 79 000 cells per cm^2 and left in the incubator at 37 °C for 24 hours. To assess the biocompatibility cells were stained with a solution of Calcein-AM (Merck Life Science, final concentration 1 μg mL^{-1}) and Ethidium Homodimer (Thermo Fisher, final concentration 10 μg mL^{-1}) in PBS and incubated at 37 °C for 10 minutes.

MTT assay. HT22 (50 000 cells per cm^2) per well were seeded into a 24-well tissue culture plate for 24 hours. Before plating, substrates were functionalized with poly-L-lysine (PLL, Merck Life Science S.r.l., Italy) 0.01% v/v (aqueous solution), incubated at 37 °C overnight and then washed three times with PBS (Merck Life Science S.r.l., Italy). A solution of MTT 3-(4,5-dimethylthiazol-2-yl)-2,5-diphenyl tetrazolium bromide (Abcam, UK) in 1× solution of

PBS (Merck Life Science S.r.l., Italy) (5 mg mL^{-1}) was added to the wells (200 μL in 1 mL of medium) and incubated at 37 °C for 4 hours. After the removal of the medium, 1 mL of DMSO (Merck Life Science S.r.l., Italy) was added to all wells and mixed thoroughly to dissolve the dark blue crystals (insoluble purple formazan formed by cleavage of the tetrazolium ring by dehydrogenase enzymes). After a 1 hour at room temperature, to ensure that all crystals were dissolved, the DMSO solution was measured spectrophotometrically using Dynatech MR580 Microelisa reader, using a test wavelength of 570 nm.

Conflicts of interest

There are no conflicts to declare.

References

1 J. Rivnay, S. Inal, A. Salleo, R. M. Owens, M. Berggren and G. G. Malliaras, *Nat. Rev. Mater.*, 2018, **3**, 1–14.
2 A. Spanu, L. Martines and A. Bonfiglio, *Lab Chip*, 2021, **21**, 795–820.
3 Z. Zhao, Z. Tian and F. Yan, *Cell Rep. Phys. Sci.*, 2023, **4**, 101673.
4 M. Sophocleous, L. Contat-Rodrigo, E. García-Breijo and J. Georgiou, *IEEE Sens. J.*, 2021, **21**, 3977–4006.
5 C. Yao, Q. Li, J. Guo, F. Yan and I.-M. Hsing, *Adv. Healthcare Mater.*, 2015, **4**, 528–533.
6 X. Gu, S. Y. Yeung, A. Chadda, E. N. Y. Poon, K. R. Boheler and I.-M. Hsing, *Adv. Biosyst.*, 2019, **3**, 1800248.
7 L. H. Jimison, S. A. Tria, D. Khodagholy, M. Gurfinkel, E. Lanzarini, A. Hama, G. G. Malliaras and R. M. Owens, *Adv. Mater.*, 2012, **24**, 5919–5923.
8 A. M. Pappa, D. Ohayon, A. Giovannitti, I. P. Maria, A. Savva, I. Uguz, J. Rivnay, I. McCulloch, R. M. Owens and S. Inal, *Sci. Adv.*, 2018, **4**, eaat0911.
9 S. Han, S. Yamamoto, A. G. Polyravas and G. G. Malliaras, *Adv. Mater.*, 2020, **32**, 2004790.
10 G. LeCroy, C. Cendra, T. J. Quill, M. Moser, R. Hallani, J. F. Ponder, K. Stone, S. D. Kang, A. Y.-L. Liang, Q. Thiburce, I. McCulloch, F. C. Spano, A. Giovannitti and A. Salleo, *Mater. Horiz.*, 2023, **10**, 2568–2578.
11 B. D. Paulsen, K. Tybrandt, E. Stavrinidou and J. Rivnay, *Nat. Mater.*, 2020, **19**, 13–26.
12 D. Ohayon, V. Druet and S. Inal, *Chem. Soc. Rev.*, 2023, **52**, 1001–1023.
13 S. Inal, G. G. Malliaras and J. Rivnay, *Nat. Commun.*, 2017, **8**, 1767.
14 S. T. Keene, C. Lubrano, S. Kazemzadeh, A. Melianas, Y. Tuchman, G. Polino, P. Scognamiglio, L. Cinà, A. Salleo, Y. van de Burgt and F. Santoro, *Nat. Mater.*, 2020, **19**, 969–973.
15 M. J. Donahue, A. Sanchez-Sanchez, S. Inal, J. Qu, R. M. Owens, D. Mecerreyes, G. G. Malliaras and D. C. Martin, *Mater. Sci. Eng., R*, 2020, **140**, 100546.
16 G. Dijk, H. J. Ruigrok and R. P. O'Connor, *Adv. Mater. Interfaces*, 2021, **8**, 2100214.
17 E. Mitraka, M. Gryszel, M. Vagin, M. J. Jafari, A. Singh, M. Warczak, M. Mitrakas, M. Berggren, T. Ederth, I. Zozoulenko, X. Crispin and E. D. Głowacki, *Adv. Sustainable Syst.*, 2019, **3**, 1800110.
18 A. Giovannitti, R. B. Rashid, Q. Thiburce, B. D. Paulsen, C. Cendra, K. Thorley, D. Moia, J. T. Mefford, D. Hanifi, D. Weiyuan, M. Moser, A. Salleo, J. Nelson, I. McCulloch and J. Rivnay, *Adv. Mater.*, 2020, **32**, 1908047.
19 J. Ehlich, L. Migliaccio, I. Sahalianov, M. Nikić, J. Brodský, I. Gablech, X. T. Vu, S. Ingebrandt and E. D. Głowacki, *J. Neural Eng.*, 2022, **19**, 036045.
20 M. Jakešová, D. H. Apaydin, M. Sytnyk, K. Oppelt, W. Heiss, N. S. Sariciftci and E. D. Głowacki, *Adv. Funct. Mater.*, 2016, **26**, 5248.
21 B. D'Autréaux and M. B. Toledano, *Nat. Rev. Mol. Cell Biol.*, 2007, **8**, 813–824.
22 H. J. Forman, M. Maiorino and F. Ursini, *Biochemistry*, 2010, **49**, 835–842.
23 K. M. Holmström and T. Finkel, *Nat. Rev. Mol. Cell Biol.*, 2014, **15**, 411–421.
24 H. Sies, *Redox Biol.*, 2017, **11**, 613–619.
25 H. Sies, *J. Biol. Chem.*, 2014, **289**, 8735–8741.
26 V. I. Lushchak, *Chem.-Biol. Interact.*, 2014, **224**, 164–175.
27 J. Nelson, *Energy Environ. Sci.*, 2023, **16**, 337.
28 A. D. L. F. Durán, A. Y.-L. Liang, I. Denti, H. Yu, D. Pearce, A. Marks, E. Penn, J. Treiber, K. Weaver, L. Turaski, I. P. Maria, S. Griggs, X. Chen, A. Salleo, W. C. Chueh, J. Nelson, A. Giovannitti and J. T. Mefford, *Energy Environ. Sci.*, 2023, **16**, 5409–5422.

